Applied Physics Express

LETTER

# Significant reduction of crack propagation in the strained SiGe/Ge(111) induced by the local growth on the depth-controlled area patterning

To cite this article: Youya Wagatsuma *et al* 2023 *Appl. Phys. Express* **16** 015502

Applied Physics Express **16**, 015502 (2023) **LETTER**
https://doi.org/10.35848/1882-0786/aca751

# Significant reduction of crack propagation in the strained SiGe/Ge(111) induced by the local growth on the depth-controlled area patterning

Youya Wagatsuma[1*], Rena Kanesawa[1], Md. Mahfuz Alam[1,2], Kazuya Okada[1], Takahiro Inoue[1], Michihiro Yamada[3], Kohei Hamaya[3,4], and Kentarou Sawano[1*]

[1]*Advanced Research Laboratories, Tokyo City University, 8-15-1 Todoroki, Setagaya-Ku, Tokyo 158-0082, Japan*
[2]*Department of Physics, University of Barishal, Barishal-8254, Bangladesh*
[3]*Center for Spintronics Research Network, Graduate School of Engineering Science, Osaka University, Toyonaka, Osaka 560-8531, Japan*
[4]*Institute for Open and Transdisciplinary Research Initiatives, Osaka University, Yamadaoka 2-1, Suita, Osaka, Japan*

*E-mail: g2191206@tcu.ac.jp; sawano@tcu.ac.jp

Received November 13, 2022; revised November 23, 2022; accepted November 29, 2022; published online December 19, 2022

We propose a method for obtaining crack-free fully-strained SiGe layers on Ge(111). To achieve the crack-free strained SiGe layers, we introduce a patterned area with a sufficient depth (step height) of more than 1 $\mu$m on Ge(111) substrates. Because of the complete suppression of the crack propagation from the SiGe layer grown on the outside of the patterned area on Ge(111), we achieve crack-free fully strained SiGe layers on the inside of the patterned area. This approach will drastically expand the applicability of the strained SiGe to the fields of Si photonics and spintronics.


A SiGe with high Ge concentrations is expected to offer various potential applications for photonic and spintronics devices on the Si platform. Particularly, various strain and band engineering are possible by utilizing SiGe/Ge heterostructures, where the Ge concentrations in SiGe and resultantly band offset as well as the strain can be arbitrarily controlled.[1–5] For instance, SiGe/Ge multi-quantum well structures are attractive for photodetectors and light-emitting devices that have been attracting increased attention in the Si photonics field.[6–12] Moreover, as high-quality ferromagnetic Heusler alloys can be epitaxially grown on SiGe(111) with high Ge concentrations,[13,14] SiGe is very important for spintronics devices. Thus far, pure spin-current transport has been observed in Ge(111) and SiGe epitaxial layers even at room temperature.[15–17] Recently, in the strained $Si_{0.1}Ge_{0.9}$ layers, we clearly observed an enhancement in the spin lifetime at room temperature,[18] meaning that the strain induced in $Si_{0.1}Ge_{0.9}$ enables us to lift the degeneracy between L-valleys in the conduction bands where the intervalley spin-flip scattering occurs. Since high-quality Ge-on-Si virtual substrates have recently become available owing to the two-step growth method,[19–23] feasibility of employment of SiGe with high Ge concentrations has remarkably increased. Toward wider applications of the SiGe/Ge heterostructures, however, epitaxial growth of high-quality SiGe with a sufficient thickness for specific applications is still an issue of great importance.

In our previous works, we investigated the critical thickness of strained SiGe layers grown on bulk Ge(111) substrates and Ge-on-Si(111) virtual substrates and found that the critical thickness is thicker for the SiGe on the bulk Ge than that on the Ge-on-Si virtual substrate.[24] Also we have shown that SiGe layers with a thickness exceeding the critical thickness possess high-density cracks all over the SiGe layer and the cracks penetrate into the underlying Ge substrates.[24,25] To avoid crack formation, we proposed a patterning method, where we grew strained SiGe layers on patterned Ge-on-Si(111) substrates.[26] Mesa patterns were formed by fully etching down the epitaxial Ge-on-Si outside of the mesa area. As a result, we succeeded in suppressing the crack formation and increasing the critical thickness of the strained SiGe layers on the mesa area. It is interesting to mention that the crack suppression completely fails if the Ge-on-Si was not fully etched down outside of the mesa area. We speculated that the cracks are generated in the SiGe on partially etched Ge outside of the mesa area and the generated cracks propagate and enter the mesa.[27] To confirm this phenomenon and to investigate the effects of the mesa step height on the crack propagation across the step, in this study, we grow strained SiGe layers on the Ge substrate which are mesa-patterned with various etching depths to clarify the crack propagation behaviors. As a result, we find that the mesa step with sufficient heights can block the propagation, leading to crack-free strained SiGe layers on Ge(111) realized on the mesa area.

The crystal growth of SiGe/Ge heterostructures was carried out using a solid source molecular beam epitaxy system with an electron beam gun and Knudsen cell for evaporation of Si and Ge, respectively. The mesa-patterning of the Ge(111) substrate was performed by the standard photolithography process and $H_2O_2$ etching of the Ge.[26,27] The etched depth $d_{etched}$ was varied from 200 nm to 1.5 $\mu$m. The mesa-pattern size was defined to be 80 $\mu$m × 80 $\mu$m as shown in Fig. 1. On the patterned Ge substrate, strained $Si_{0.2}Ge_{0.8}$ layers with thicknesses of 200, 250, and 400 nm were grown at 350 °C where the growth rates of Si and Ge were 0.2 and 0.8 Å $s^{-1}$, respectively. Surface morphologies were evaluated with a laser microscope (KEYENCE VK-X150). Local strain states were evaluated by micro-Raman measurement with back-scattering geometry, where a 532 nm laser with a beam spot of 1 $\mu m^2$ was incident on a selected point of the sample surface.

Figure 2 shows laser microscope (LM) images of the strained $Si_{0.2}Ge_{0.8}$ layers with a thickness of 250 nm grown on the patterned Ge substrates with $d_{etched}$ of (a) 200 nm, (b) 300 nm and (c) 1 $\mu$m. It is clearly observed that the line-shaped ridge roughness is formed on the SiGe surfaces both inside and outside of the mesa for $d_{etched}$ of 200 and 300 nm. In our previous study, cross-sectional TEM observation has shown that the ridge roughness is caused by cracks that are generated on equivalent (111) planes within the SiGe layers and penetrating into the underlying Ge substrates.[25] This means that high-density cracks are generated all over the sample surface despite the mesa-patterning of the Ge

 

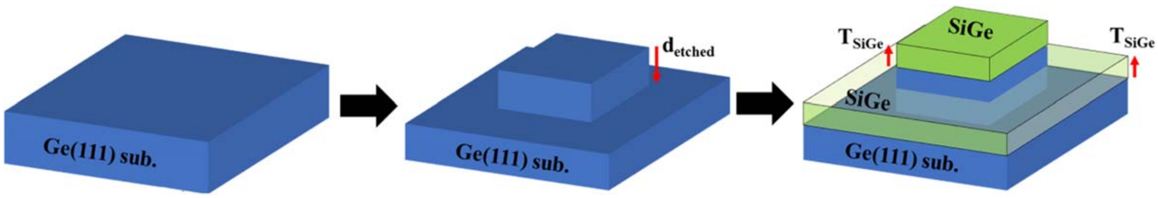


**Fig. 1.** (Color online) Fabrication procedures of strained SiGe on the patterned Ge(111) substrates where Ge layers were etched down with various thicknesses.

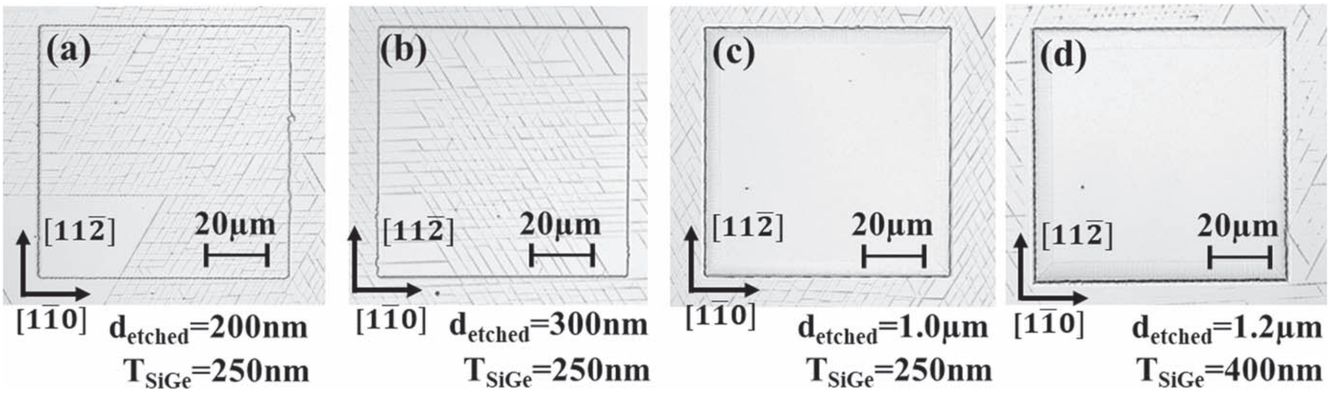


**Fig. 2.** Laser microscope surface images of the (a), (b) and (c) 250 nm and (d) 400 nm thick strained $Si_{0.2}Ge_{0.8}$ layers grown on patterned Ge(111) substrates where Ge layer was etched down with various thicknesses.

substrate. It is seen that each crack is continuously connected at the boundary of the mesa. This behavior is almost the same as observed for the SiGe layers grown on the mesa-patterned Ge-on-Si substrate where the Ge layer outside of the mesa was partially etched and resultantly a Ge thin layer remains on the Si outside of the mesa.

By contrast, for the sample with $d_{etched}$ of 1 $\mu$m [Fig. 2(c)] it is obviously found that the mesa area is completely free from such cracks while high-density cracks do cover all the area outside of the mesa. This result obviously demonstrates the finding that the patterning of the Ge substrate is effective to suppress the generation of the cracks in the strained SiGe layer grown on the Ge and that this effect works only when the mesa-patterning step height is sufficiently large.

From the above results, we discuss mechanisms of the crack formation and its suppression by the patterning as follows. Considering the fact that the mesa area is free from the cracks for the sample with $d_{etched}$ of 1 $\mu$m, we can assume that a source of crack generation does not exist within the $80 \times 80\ \mu m^2$ mesa area. A crack is initially generated outside of the mesa and the generated crack rapidly propagates. During the propagation, the crack is multiplied, leading to the formation of a crack network over the SiGe layer outside of the mesa. When some cracks reach the mesa boundary, the crack propagation is blocked by the sufficiently high mesa step. If the step height is not high enough, the propagation proceeds across the mesa boundary, which leads to the formation of the crack network inside the mesa area as well as outside of the mesa. Detailed investigations of mechanisms of the crack propagation blocking due to the step are now underway.

Furthermore, we attempted to increase the SiGe thickness up to 400 nm which is far beyond the critical thickness, which is around 100 nm.[24] Figure 2(d) shows an LM image for the 400 nm SiGe grown on the patterned Ge(111) substrate with $d_{etched}$ of 1.2 $\mu$m. It is remarkable that no crack is found on the mesa area and high-density cracks appear outside of the mesa as observed for the 250 nm thick SiGe [Fig. 2(c)].

Line densities of the cracks were estimated from LM images for all samples fabricated in this study. Figure 3 summarizes the densities of the cracks (a) inside and (b) outside of the mesa area as a function of $d_{etched}$ for the strained $Si_{0.2}Ge_{0.8}$ layers with various thicknesses. As observed above, for $d_{etched}$ larger than 1.0 $\mu$m, the cracks are absent in the mesa area both for the 250 and 400 nm thick SiGe layers, which corresponds to plots at 0 $\mu m^{-1}$ [Fig. 3(a)]. With $d_{etched}$ smaller than 1.0 $\mu$m, cracks are observed in the mesa area with densities from 0.1 to 0.4 $\mu m^{-1}$. These densities inside of the mesa area [Fig. 3(a)] are almost the same as the densities outside of the mesa [Fig. 3(b)], which means that the mesa step hardly hinders the crack propagation at the boundary, resulting in almost the same densities between the inside and outside of the mesa. It should be noted that densities outside of the mesa for the samples with $d_{etched}$ larger than 1.0 $\mu$m are similar to those with $d_{etched}$ smaller than 1.0 $\mu$m, which means the densities outside of the mesa are not influenced by the presence of the mesa even though its height is large enough to block the crack propagation. It is also notable in Fig. 3(b) that the 200 nm thick SiGe exhibits a smaller density than the 250 nm thick SiGe layers and that the density for the 400 nm thick SiGe is similar to that of the 250 nm thick SiGe. These results imply that the density increase with the SiGe thickness up to 250 nm and may saturate beyond 250 nm.

Strain states were characterized for the 250 nm thick SiGe with $d_{etched}$ of 1.0 $\mu$m with micro-Raman measurements. Figure 4 shows Raman spectra obtained from the (a) inside and (b) outside of the mesa-pattern as indicated in the inset LM image. As a reference, a spectrum of the bulk Ge is

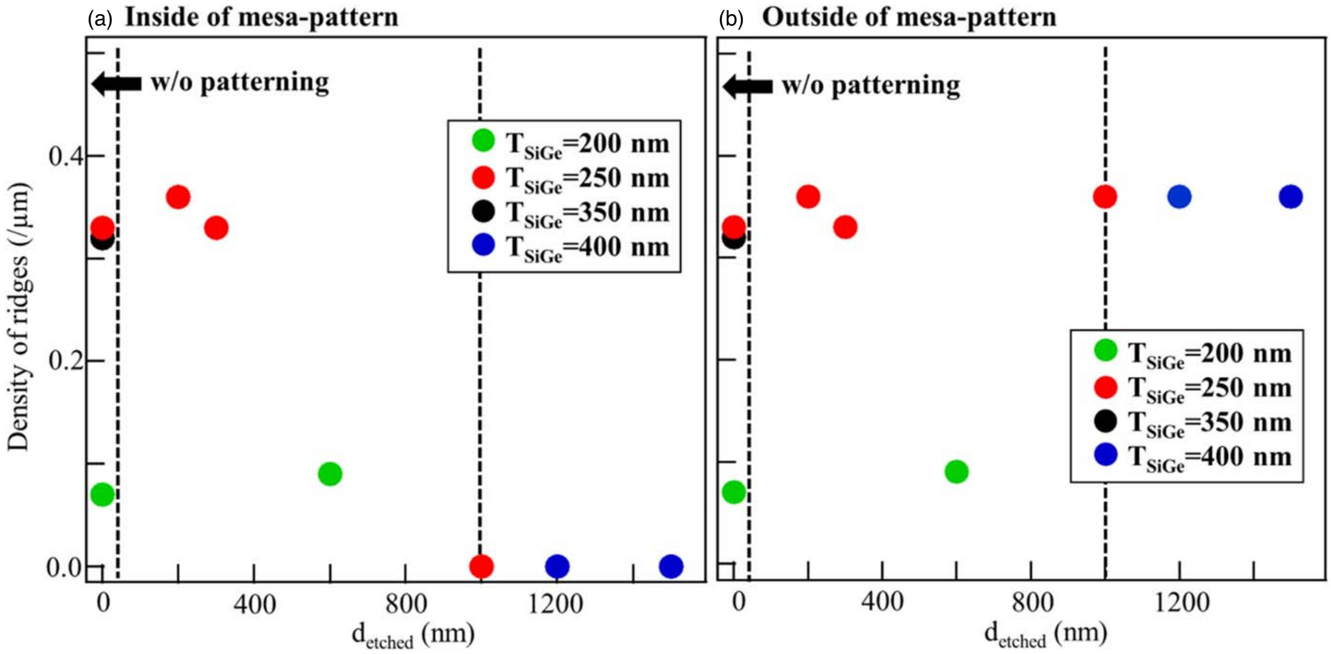


**Fig. 3.** (Color online) Density of ridges for (a) inside and (b) outside of mesa-pattern in various thick $Si_{0.2}Ge_{0.8}$ layers on patterned and un-patterned Ge(111) substrates where Ge layers were etched down with various thicknesses.

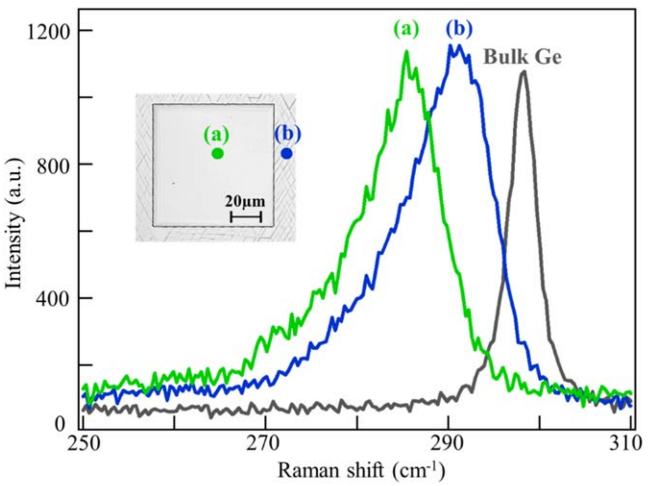


**Fig. 4.** (Color online) Raman spectra of (a) bulk Ge and 250 nm thick $Si_{0.2}Ge_{0.8}$ layers of (b) inside and (b) outside of mesa-pattern.

shown together. We can find Ge–Ge mode peaks from the strained SiGe layer while no peak from the underlying Ge substrate is found as the thickness of the SiGe is large enough to absorb the laser light. It is clearly found that peak values differ significantly between the inside and outside of the mesa-pattern, meaning that the strain states are different. The observed peak shift to higher wavenumbers corresponds to partial relaxation of the originally induced tensile strain.

The SiGe outside of the mesa is considered to relax through the crack formation. By contrast, cracks were not formed inside the mesa area, as shown, leading to the completely strained SiGe layer in the mesa area. We can say that crack formation and associated relaxation can be suppressed by the mesa-patterning with sufficient step height.

We studied crack formation mechanisms in the tensile-strained SiGe layers grown on patterned Ge substrates, where square-shaped mesa areas were defined with various etching depths. High-density cracks were formed in the SiGe layer both inside and outside of the mesa area in the case of the etching depth of less than 1 $\mu$m. In contrast, for the case of etching depth of more than 1 $\mu$m, crack-free SiGe layers were obtained in the mesa areas whereas the high-density cracks appear outside of the mesa areas, meaning that propagation of the generated cracks was completely blocked by the mesa step with sufficient heights.

We can speculate that the crack generation takes place at some point far away from the mesa, presumably near edge regions of the sample chip. Any crack generation source does not exist in at least the mesa area of $80 \times 80\ \mu m^2$. By blocking the crack propagation coming from the edge regions, we can form a crack-free strained SiGe mesa that is large enough for device fabrications and integrations. Based on these findings, we can apply this patterning method to the SiGe growth on Ge-on-Si and/or Ge-on-Insulators for strained SiGe-based high-performance devices on the Si platform.

**Acknowledgements** This work was supported in part by JST SPRING, Grant No. JAMJSP2118 and Grant-in-Aid for Scientific Research (Nos. 19H02175, 19H05616 and 20K21009) from MEXT, Japan.

1) C. W. Leitz, M. T. Currie, M. L. Lee, Z.-Y. Cheng, D. A. Antoniadis, and E. A. Fitzgerald, J. Appl. Phys. **92**, 3745 (2002).
2) A. Toriumi and T. Nishimura, Jpn. J. Appl. Phys. **57**, 010101 (2018).
3) O. A. Mironov et al., Thin Solid Films **557**, 329 (2014).
4) T. Tanaka, Y. Hoshi, K. Sawano, N. Usami, Y. Shiraki, and K. M. Itoh, Appl. Phys. Lett. **100**, 222102 (2012).
5) M. L. Lee, E. A. Fitzgerald, M. T. Bulsara, M. T. Currie, and A. Lochtefeld, J. Appl. Phys. **97**, 011101 (2005).
6) X.-C. Liu and D. R. Leadley, J. Phys. D: Appl. Phys. **43**, 505303 (2010).
7) Y. Busby et al., Phys. Rev. B **82**, 205317 (2010).
8) J. Frigerio, P. Chaisakul, D. Marris-Morini, M.-S. Rouifed, S. Cecchi, D. Chrastina, G. Isella, and L. Vivien, ECS Trans. **64**, 761 (2014).
9) C. Lq, Y. Chen, and C. Li, Optoelectron. Lett. **10**, 213 (2014).
10) G.-E. Chang, S.-W. Chen, and H. H. Cheng, Opt. Express **24**, 17562 (2016).
11) G. Lin, N. Chen, L. Zhang, Z. Huang, W. Huang, J. Wang, J. Xu, S. Chen, and C. Li, Materials **9**, 803 (2016).

12) Y. Yamamoto, O. Skibitzki, M. Andreas Schubert, M. Scuderi, F. Reichmann, M. H. Zöllner, M. D. Seta, G. Capellini, and B. Tillack, Jpn. J. Appl. Phys. **59** (2020).
13) K. Hamaya, Y. Fujita, M. Yamada, M. Kawano, S. Yamada, and K. Sawano, J. Phys. D: Appl. Phys. **51**, 393001 (2018).
14) M. Yamada, T. Naito, M. Tsukahara, S. Yamada, K. Sawano, and K. Hamaya, Semicond. Sci. Technol. **33**, 114009 (2018).
15) M. Yamada, F. Kuroda, M. Tsukahara, S. Yamada, T. Fukushima, K. Sawano, T. Oguchi, and K. Hamaya, NPG Asia Mater. **12**, 47 (2020).
16) T. Naito, M. Yamada, M. Tsukahara, S. Yamada, K. Sawano, and K. Hamaya, Appl. Phys. Express **11**, 053006 (2018).
17) T. Naito, M. Yamada, S. Yamada, K. Sawano, and K. Hamaya, Phys. Rev. Appl. **13**, 054025 (2020).
18) T. Naito, M. Yamada, Y. Wagatsuma, K. Sawano, and K. Hamaya, Phys. Rev. Applied **18**, 024005 (2022).
19) K. Sawano et al., Thin Solid Films **557**, 76 (2014).
20) K. Sawano, Y. Hoshi, S. Kubo, K. Arimoto, J. Yamanaka, K. Nakagawa, K. Hamaya, M. Miyao, and Y. Shiraki, Thin Solid Films **613**, 24 (2016).
21) M. M. Alam, Y. Hoshi, and K. Sawano, Semicond. Sci. Technol. **33**, 124008 (2018).
22) V. H. Nguyen, A. Dobbie, M. Myronov, and D. R. Leadley, J. Appl. Phys. **114**, 154306 (2013).
23) A. Ghosh, M. B. Clavel, P. D. Nguyen, M. A. Meeker, G. A. Khodaparast, R. J. Bodnar, and M. K. Hudait, AIP Adv. **7**, 095214 (2017).
24) M. M. Alam, Y. Wagatsuma, K. Okada, Y. Hoshi, M. Yamada, K. Hamaya, and K. Sawano, Appl. Phys. Express **12**, 081005 (2019).
25) Y. Wagatsuma, M. M. Alam, K. Okada, Y. Hoshi, M. Yamada, K. Hamaya, and K. Sawano, Mat. Sci. Semicond. Proc. **117**, 105153 (2020).
26) Y. Wagatsuma, M. M. Alam, K. Okada, M. Yamada, K. Hamaya, and K. Sawano, Appl. Phys. Express **14**, 025502 (2021).
27) Y. Wagatsuma, M. M. Alam, K. Okada, R. Kanesawa, M. Yamada, K. Hamaya, and K. Sawano, J. Cryst. Growth **589**, 126672 (2022).